


---

This is the **accepted version** of the journal article:

Stef Haesen; Jonas J. Lembrechts; Pieter De Frenne; [et al.]. «ForestClim-Bioclimate variables for microclimate temperatures of European forests». *Global Change Biology*, Vol. 29, issue 11 (June 2023), p. 2886-2892. DOI 10.1111/gcb.16678

---

This version is available at <https://ddd.uab.cat/record/287589>

under the terms of the  **COPYRIGHT** license

# ForestClim—Bioclimatic variables for microclimate temperatures of European forests

Stef Haesen<sup>1</sup>, Jonas J. Lembrechts<sup>2</sup>, Pieter De Frenne<sup>3</sup>, Jonathan Lenoir<sup>4</sup>, Juha Aalto<sup>5</sup>, Michael B. Ashcroft<sup>6</sup>, Martin Kopecký<sup>7,8</sup>, Miska Luoto<sup>9</sup>, Ilya Maclean<sup>10</sup>, Ivan Nijs<sup>2</sup>, Pekka Niittynen<sup>9</sup>, Johan van den Hoogen<sup>11</sup>, Nicola Arriga<sup>12</sup>, Josef Brůna<sup>7</sup>, Nina Buchmann<sup>11</sup>, Marek Čiliak<sup>13</sup>, Alessio Collalti<sup>14</sup>, Emiel De Lombaerde<sup>3</sup>, Patrice Descombes<sup>15,16</sup>, Mana Gharun<sup>11</sup>, Ignacio Goded<sup>12</sup>, Sanne Govaert<sup>3</sup>, Caroline Greiser<sup>17</sup>, Achim Grelle<sup>18</sup>, Carsten Gruening<sup>12</sup>, Lucia Hederová<sup>7</sup>, Kristoffer Hylander<sup>17</sup>, Jürgen Kreyling<sup>19</sup>, Bart Kruijt<sup>20</sup>, Martin Macek<sup>7</sup>, František Máliš<sup>21</sup>, Matěj Man<sup>7</sup>, Giovanni Manca<sup>12</sup>, Radim Matula<sup>8</sup>, Camille Meeussen<sup>3</sup>, Sonia Merinero<sup>17,22</sup>, Stefano Minerbi<sup>23</sup>, Leonardo Montagnani<sup>23,24</sup>, Lena Muffler<sup>25</sup>, Romà Ogaya<sup>26</sup>, Josep Penuelas<sup>26,27</sup>, Roman Plichta<sup>28</sup>, Miguel Portillo-Estrada<sup>2</sup>, Jonas Schmeddes<sup>19</sup>, Ankit Shekhar<sup>11</sup>, Fabien Spicher<sup>4</sup>, Mariana Ujházyová<sup>13</sup>, Pieter Vangansbeke<sup>3</sup>, Robert Weigel<sup>25</sup>, Jan Wild<sup>7</sup>, Florian Zellweger<sup>29</sup>, Koenraad Van Meerbeek<sup>1</sup>

*\*Corresponding author, OrcID = <https://orcid.org/0000-0002-4491-4213>, [stef.haesen@kuleuven.be](mailto:stef.haesen@kuleuven.be), +32 16 32 24 67*

<sup>1</sup>*Department of Earth and Environmental Sciences, Celestijnenlaan 200E, 3001 Leuven, Belgium;*

<sup>2</sup>*Research Group PLECO (Plants and Ecosystems), University of Antwerp, 2610 Wilrijk, Belgium; <sup>3</sup>Forest & Nature Lab, Department of Environment, Ghent University, Geraardsbergsesteenweg 267, 9090 Melle-Gontrode, Belgium; ; <sup>4</sup>UMR CNRS 7058 ‘Ecologie et Dynamique des Systèmes Anthropisés’ (EDYSAN), Univ. de Picardie Jules Verne, Amiens, France; <sup>5</sup>Finnish Meteorological Inst., P.O. Box 503, FI-00101 Helsinki, Finland; <sup>6</sup>Centre for Sustainable Ecosystem Solutions, School of Biological Sciences, University of Wollongong, Wollongong, Australia; <sup>7</sup>Institute of Botany of the Czech Academy of Sciences, Zámek 1, CZ-25243, Průhonice, Czech Republic; <sup>8</sup>Faculty of Forestry and Wood Sciences, Czech University of Life Sciences Prague, Kamýcká 129, CZ-165 21, Prague 6 - Suchbátka, Czech Republic; <sup>9</sup>Dept of Geosciences and Geography, Gustaf Hållströmin katu 2a, FIN-00014 Univ. of Helsinki, Finland;*

<sup>10</sup>*Environment and Sustainability Institute, University of Exeter, Penryn Campus, Penryn, UK, TR10 9FE; <sup>11</sup>Department of Environmental Systems Science, ETH Zurich, Universitaetstrasse 2, 8092 Zurich, Switzerland; <sup>12</sup>European Commission, Joint Research Centre (JRC), Ispra, Italy; <sup>13</sup>Faculty of Ecology and Environmental Sciences, Technical University in Zvolen, T.G.Masaryka 24, 960 01 Zvolen, Slovakia; <sup>14</sup>Institute for Agriculture and Forestry Systems in the Mediterranean, National Research Council of Italy (CNR-ISAFO), Perugia, Italy; <sup>15</sup>Dept. of Ecology & Evolution, University of Lausanne, 1015 Lausanne, Switzerland; <sup>16</sup>Musée et Jardins botaniques Cantonaux, 1007 Lausanne, Switzerland; <sup>17</sup>Department of Ecology, Environment and Plant Sciences and Bolin Centre for Climate Research, Stockholm University, 106 91 Stockholm, Sweden; <sup>18</sup>Department of Ecology, Swedish University of Agricultural Sciences, Uppsala, Sweden; <sup>19</sup>Experimental Plant Ecology, Institute of Botany and*

Landscape Ecology, University of Greifswald, D-17487 Greifswald, Germany; <sup>20</sup>Wageningen University and Research, Wageningen, Netherlands; <sup>21</sup>Faculty of Forestry, Technical University in Zvolen, T.G.Masaryka 24, 960 01 Zvolen, Slovakia; <sup>22</sup>Department of Plant Biology and Ecology, University of Seville, Apartado 1095, 41080 Seville, Spain; <sup>23</sup>Forest Services, Autonomous Province of Bolzan, 39100 Bolzano, Italy; <sup>24</sup>Faculty of Science and Technology, Free University of Bolzano, 39100 Bolzano, Italy; <sup>25</sup>Plant Ecology, Albrecht-von-Haller-Institute for Plant Sciences, Georg-August University of Goettingen, Untere Karspuele 2, 37073 Goettingen, Germany; <sup>26</sup>CSIC, Global Ecology Unit CREA- CSIC- UAB, Bellaterra, 08193, Catalonia, Spain; <sup>27</sup>CREAF, Cerdanyola del Vallès 08193, Catalonia, Spain; <sup>28</sup>Department of Forest Botany, Dendrology and Geobiocoenology, Mendel University in Brno, Czech Republic; <sup>29</sup>Swiss Federal Institute for Forest, Snow and Landscape Research WSL, Birmensdorf, Switzerland

## OrcIDs

Jonas J. Lembrechts: <a href="https://orcid.org/0000-0002-1933-0750">https://orcid.org/0000-0002-1933-0750</a>	Jürgen Kreyling: <a href="https://orcid.org/0000-0001-8489-7289">https://orcid.org/0000-0001-8489-7289</a>
Pieter De Frenne: <a href="https://orcid.org/0000-0002-8613-0943">https://orcid.org/0000-0002-8613-0943</a>	Bart Kruijt: <a href="https://orcid.org/0000-0002-6186-1731">https://orcid.org/0000-0002-6186-1731</a>
Juha Aalto: <a href="https://orcid.org/0000-0001-6819-4911">https://orcid.org/0000-0001-6819-4911</a>	Martin Macek: <a href="https://orcid.org/0000-0002-5609-5921">https://orcid.org/0000-0002-5609-5921</a>
Martin Kopecký: <a href="https://orcid.org/0000-0002-1018-9316">https://orcid.org/0000-0002-1018-9316</a>	František Máliš: <a href="https://orcid.org/0000-0003-2760-6988">https://orcid.org/0000-0003-2760-6988</a>
Jonathan Lenoir: <a href="https://orcid.org/0000-0003-0638-9582">https://orcid.org/0000-0003-0638-9582</a>	Matěj Man: <a href="https://orcid.org/0000-0002-4557-8768">https://orcid.org/0000-0002-4557-8768</a>
Miska Luoto: <a href="https://orcid.org/0000-0001-6203-5143">https://orcid.org/0000-0001-6203-5143</a>	Giovanni Manca: <a href="https://orcid.org/0000-0002-9376-0310">https://orcid.org/0000-0002-9376-0310</a>
Ilya Maclean: <a href="https://orcid.org/0000-0001-8030-9136">https://orcid.org/0000-0001-8030-9136</a>	Radim Matula: <a href="https://orcid.org/0000-0002-7460-0100">https://orcid.org/0000-0002-7460-0100</a>
Ivan Nijs: <a href="https://orcid.org/0000-0003-3111-680X">https://orcid.org/0000-0003-3111-680X</a>	Camille Meeussen: <a href="https://orcid.org/0000-0002-5869-4936">https://orcid.org/0000-0002-5869-4936</a>
Pekka Niittynen: <a href="https://orcid.org/0000-0002-7290-029X">https://orcid.org/0000-0002-7290-029X</a>	Sonia Merinero: <a href="https://orcid.org/0000-0002-1405-6254">https://orcid.org/0000-0002-1405-6254</a>
Johan van den Hoogen: <a href="https://orcid.org/0000-0001-6624-8461">https://orcid.org/0000-0001-6624-8461</a>	Stefano Minerbi: <a href="https://orcid.org/0000-0002-6620-2735">https://orcid.org/0000-0002-6620-2735</a>
Nicola Arriga: <a href="https://orcid.org/0000-0001-5321-3497">https://orcid.org/0000-0001-5321-3497</a>	Leonardo Montagnani: <a href="https://orcid.org/0000-0003-2957-9071">https://orcid.org/0000-0003-2957-9071</a>
Josef Brůna: <a href="https://orcid.org/0000-0002-4839-4593">https://orcid.org/0000-0002-4839-4593</a>	Lena Muffler: <a href="https://orcid.org/0000-0001-8227-7297">https://orcid.org/0000-0001-8227-7297</a>
Nina Buchmann: <a href="https://orcid.org/0000-0003-0826-2980">https://orcid.org/0000-0003-0826-2980</a>	Romà Ogaya: <a href="http://orcid.org/0000-0003-4927-8479">http://orcid.org/0000-0003-4927-8479</a>
Marek Čiliak: <a href="https://orcid.org/0000-0002-6720-9365">https://orcid.org/0000-0002-6720-9365</a>	Josep Penuelas: <a href="https://orcid.org/0000-0002-7215-0150">https://orcid.org/0000-0002-7215-0150</a>
Alessio Collalti: <a href="https://orcid.org/0000-0002-4980-8487">https://orcid.org/0000-0002-4980-8487</a>	Roman Plichta: <a href="https://orcid.org/0000-0003-2442-8522">https://orcid.org/0000-0003-2442-8522</a>
Emiel De Lombaerde: <a href="https://orcid.org/0000-0002-0050-2735">https://orcid.org/0000-0002-0050-2735</a>	Miguel Portillo-Estrada: <a href="https://orcid.org/0000-0002-0348-7446">https://orcid.org/0000-0002-0348-7446</a>
Patrice Descombes: <a href="https://orcid.org/0000-0002-3760-9907">https://orcid.org/0000-0002-3760-9907</a>	Ankit Shekhar: <a href="https://orcid.org/0000-0003-0802-2821">https://orcid.org/0000-0003-0802-2821</a>
Mana Gharun: <a href="https://orcid.org/0000-0003-0337-7367">https://orcid.org/0000-0003-0337-7367</a>	Fabien Spicher: <a href="https://orcid.org/0000-0002-9999-955X">https://orcid.org/0000-0002-9999-955X</a>
Ignacio Goded: <a href="https://orcid.org/0000-0002-1912-325X">https://orcid.org/0000-0002-1912-325X</a>	Mariana Ujházyová: <a href="https://orcid.org/0000-0002-5546-1547">https://orcid.org/0000-0002-5546-1547</a>
Sanne Govaert: <a href="https://orcid.org/0000-0002-8939-1305">https://orcid.org/0000-0002-8939-1305</a>	Pieter Vangansbeke: <a href="https://orcid.org/0000-0002-6356-2858">https://orcid.org/0000-0002-6356-2858</a>
Caroline Greiser: <a href="https://orcid.org/0000-0003-4023-4402">https://orcid.org/0000-0003-4023-4402</a>	Robert Weigel: <a href="https://orcid.org/0000-0001-9685-6783">https://orcid.org/0000-0001-9685-6783</a>
Achim Grelle: <a href="https://orcid.org/0000-0003-3468-9419">https://orcid.org/0000-0003-3468-9419</a>	Wild Jan: <a href="https://orcid.org/0000-0003-3007-4070">https://orcid.org/0000-0003-3007-4070</a>
Carsten Gruening: <a href="https://orcid.org/0000-0002-6169-2827">https://orcid.org/0000-0002-6169-2827</a>	Florian Zellweger: <a href="https://orcid.org/0000-0003-1265-9147">https://orcid.org/0000-0003-1265-9147</a>
Lucia Hederová: <a href="https://orcid.org/0000-0003-1283-0952">https://orcid.org/0000-0003-1283-0952</a>	Koenraad Van Meerbeek: <a href="https://orcid.org/0000-0002-9260-3815">https://orcid.org/0000-0002-9260-3815</a>
Kristoffer Hylander: <a href="https://orcid.org/0000-0002-1215-2648">https://orcid.org/0000-0002-1215-2648</a>	

## ABSTRACT

Ecological research heavily relies on coarse-gridded climate data based on standardised temperature measurements recorded at 2 m height in open landscapes. However, many organisms experience environmental conditions that differ substantially from those captured by these macroclimatic (i.e. free-air) temperature grids. In forests, the tree canopy functions as a thermal insulator and buffers sub-canopy microclimatic conditions, thereby affecting biological and ecological processes. To improve the assessment of climatic conditions and climate change-related impacts on forest-floor biodiversity and functioning, high-resolution temperature grids reflecting forest microclimates are thus urgently needed. Combining more than 1,200 time series of *in situ* near-surface forest temperature with topographical, biological and macroclimatic variables in a machine learning model, we predicted the mean monthly offset between sub-canopy temperature at 15 cm above the surface and free-air temperature over the period 2000-2020 at a spatial resolution of 25 m across Europe. This offset was used to evaluate the difference between micro- and macroclimate across space and seasons and finally enabled us to calculate mean annual and monthly temperatures for European forest understories. We found that sub-canopy air temperatures differ substantially from free-air temperatures, being on average **0.6°C (standard deviation  $\pm$  0.8°C)** lower in summer and **1.0°C higher ( $\pm$  1.5°C)** in winter across Europe. Additionally, our high-resolution maps expose considerable microclimatic variation within landscapes, not captured by the gridded macroclimatic products. The provided forest sub-canopy temperature maps will enable future research to model below-canopy biological processes and patterns, as well as species distributions more accurately.

**Keywords:** biodiversity, boosted regression trees, climate change, ecosystem processes, forest microclimate, SoilTemp, species distributions, thermal buffering

## INTRODUCTION

Climate change is having profound impacts on Earth's biodiversity and ecosystem functioning (Lenoir et al., 2020; Pecl et al., 2017; Scheffers et al., 2016). Ecological research assessing the consequences of climate change is, however, largely based on coarse-gridded climate data of approximately 1 km<sup>2</sup> or more (Lenoir et al., 2013; Willis & Bhagwat, 2009), such as WorldClim (1 km<sup>2</sup>; Fick & Hijmans, 2017), CHELSA (1 km<sup>2</sup>; Karger et al., 2017) and TerraClimate (16 km<sup>2</sup>; Abatzoglou, Dobrowski, Parks, & Hegewisch, 2018). For the terrestrial parts of the globe, these climatic grids are derived from standardised meteorological stations recording weather conditions at approximately 2 meters height in open and windy habitats to remove microclimatic effects (Jarraud, 2008). Consequently, these grids are representative for long-term free-air temperatures (the "macroclimate") in open ecosystems. However, many organisms experience temperatures that substantially deviate from those captured by macroclimatic grids (Bramer et al., 2018; De Frenne et al., 2019). These so-called microclimatic temperatures play a crucial role in dictating biological and ecological processes close to the ground surface such as vegetation, carbon and nutrient dynamics and species distributions (Lembrechts, Nijs, & Lenoir, 2018; Nilsson & Wardle, 2005; Perry, 1994).

The available coarse-grained macroclimate data have been shown to fall short in its ability to capture small-scale biological and physical processes close to the ground surface (Lembrechts et al., 2019; Lenoir, Hattab, & Pierre, 2017). For example, small herbaceous plants are responding to microclimatic temperatures near the ground surface rather than free-air temperatures at 2 m height, and it has been shown that the currently available macroclimate data inaccurately reflect the distribution of these species (Lembrechts et al., 2019). This may lead to erroneous predictions of species range dynamics (Lembrechts et al., 2018). The core of this problem is twofold. First, macroclimatic grids do not consider many climate-forcing factors operating near the ground surface. The ground and canopy surfaces absorb solar radiation and low wind speeds reduce thermal mixing of the air, leading to significant fine-scale vertical and horizontal variation in air temperature (Geiger, 1950; Monin & Obukhov, 1954; Richardson, 1922). Second, data readily available from global macroclimatic grids consider the Earth to be a homogeneous surface of short vegetation with shading consistent with that of a weather station. However, microclimates are arguably nowhere more evident than in forests, where the amount of sunlight reaching the ground surfaces and absorbed by leaves varies substantially owing to the structural complexity of forest canopies and significant variation in evapotranspirative cooling (Bramer et al., 2018; De Frenne et al., 2019; Lenoir et al., 2017). Furthermore, landscapes characterized by considerable topographic variation (e.g. slope, aspect, elevation) have shown to harbour ample microclimatic variation (Lenoir et al., 2013; Macek, Kopecký,

& Wild, 2019) due to the effect of topography on processes such as cold-air drainage, incident solar radiation and hydrology.

Although not a new discipline, microclimate ecology has gained renewed interest over the past years (Bramer et al., 2018; De Frenne et al., 2021), providing the scientific community with many insights on the processes underlying microclimate variability, especially related to the implications of climate change. For example, several mechanistic models are available to derive microclimatic temperatures (Kearney & Porter, 2017; Kearney et al., 2014; Maclean, 2019). Other studies make use of an empirical design, in which a network of microclimate temperature loggers is installed within a certain region to cover large environmental gradients (Frey et al., 2016; George, Thompson, & Faaborg, 2015; Govaert et al., 2020; Greiser, Meineri, Luoto, Ehrlén, & Hylander, 2018; Macek et al., 2019; Meeussen et al., 2021). Nonetheless, when moving to a continental extent, these methods often reach their limits. Although mechanistic models are capable of making accurate predictions at high spatiotemporal resolution across restricted spatial extents, they struggle to do this over large spatial extents, as the processes must be modelled in hourly time-steps and are thus more computationally intensive than their statistical counterparts (Maclean, Mosedale, & Bennie, 2019). Moreover, the unpredictable nature of wind gusts underneath heterogeneous forest canopies and the effects of these on temperature gradients, make it challenging to develop mechanistic models of below-canopy microclimates (Landuyt et al., 2018). On the other hand, empirical data from regional logger networks had not yet been combined within one database until very recently (Lembrechts et al., 2020). To better model ecosystem functioning and predict the effects of climate change on organisms living close to the Earth's surface, gridded microclimate data with a broad geographical extent are thus urgently needed (Körner & Hiltbrunner, 2018; Lembrechts & Lenoir, 2020; Zellweger et al., 2019). Yet, the spatiotemporal resolution used to define microclimate is organism specific (Potter, Woods, & Pincebourde, 2013) and fractal by nature. This means that the fractal dimension, in terms of spatiotemporal resolution, of microclimate as experienced by understory plants, for instance, might be orders of magnitude larger than the fractal dimension of microclimate as experienced by smaller organisms, like insects living in tree holes or dead wood (Pincebourde & Woods, 2020).

To help fill this critical knowledge gap, the SoilTemp global database of soil and near-surface temperature time series has recently been launched (Lembrechts et al., 2020), collecting *in situ* temperature logger data from regional microclimate logger networks in various habitats across the globe. The currently available time series from **1,273** aboveground temperature sensors across European forests provide a unique opportunity to accurately predict sub-canopy forest temperature at a continental scale and at a spatial resolution that matters for organisms living in the forest understory. Here, given our focus on the forest floor, we decided to work with a spatial resolution of

25 m. Not only for practical reasons (i.e. the resolution at which predictor variables are available at a continental extent), but also for ecological reasons as this is the scale at which both foresters (i.e. forest inventories usually use plots ranging between 625 and 1,000 m<sup>2</sup>) and botanists (i.e. forest vegetation surveys usually use 100 to 500 m<sup>2</sup> plots) work to describe the forest understory in the field. For this, we calculated the mean monthly temperature offset between microclimate temperature, based on *in situ* temperature measurements from the SoilTemp database (Lembrechts et al., 2020), and macroclimate temperature, based on **EOBS data (Cruz-alonso et al., 2022)**. This offset was then related to different variables (i.e. topographical, biological and macroclimatic) to quantify the difference between micro- and macroclimate across space and seasons and to derive gridded microclimate products that are meaningful for studying biodiversity on the forest floor. Moreover, the offset enables us to (i) model average sub-canopy temperatures over a 20-year period and (ii) quantify the buffering capacities of forests across Europe, where buffering is defined as a dampening of the macroclimate, such that temporal fluctuations related to the macroclimate still exist, yet much less pronounced than outside of the forest (De Frenne et al., 2021).

## METHODS

### Data acquisition

*In situ* microclimatic temperature measurements were compiled in SoilTemp, a global database of soil and near-surface air temperature measurements combining both published and unpublished data sources (Lembrechts et al., 2020). First, we only included measurement locations within European mainland forest habitats, defined as all tree elements detectable from multispectral high resolution (20 m) satellite (Sentinel-2, Landsat 8) imagery (European Union, 2020) in all 27 EU countries, plus Albania, Bosnia and Herzegovina, Kosovo, Liechtenstein, Montenegro, North Macedonia, Norway, Serbia, the United Kingdom and Switzerland. Second, we selected near-surface air temperature measurements at a height between 0-100 cm above ground from time series spanning at least one month and a temporal resolution of less than four hours. Measurements taken at the same location, but at different heights, were included as separate data points while keeping track of logger ID to account for potential pseudo-replication issues (i.e. keeping data with the same logger ID either in the training data or in the testing data for cross-validation purposes). This resulted in **1,273** time series at **1,197** locations, extending over the period from 2000 to 2020 and geographically spanning a latitudinal gradient over Europe from Portugal (38.54N 8.00W) to Sweden (64.11N 19.45E) and a longitudinal gradient from Portugal (38.64N 8.60W) to Finland (62.33N 30.37E; Figure S1a). Note that different sensor and shielding combinations were used within the input data and that they might contribute to errors in the model (Table S1). However, experimental research has shown that such errors are relatively small in shaded environments such as forests (Maclean et al., 2021), an order of magnitude smaller than the measured offsets.

Next, we aggregated the time series, usually available at hourly or sub-daily (e.g. every two or four hours) native resolutions, to mean monthly temperatures, after visually checking each time series for outliers and erroneous data. We further only selected months with at least 28 days of data, resulting in a cumulative **25,160** months of near-surface air temperature (Table S2).

### Offset calculation

We derived a monthly temperature offset value between microclimate (i.e. sub-canopy) and macroclimate (i.e. free-air) temperature measurements ( $\Delta T = \text{sub-canopy } T^{\circ}\text{C} - \text{free-air } T^{\circ}\text{C}$ ) in order to relate this  $\Delta T$  to different explanatory variables and quantify the difference between micro- and macroclimate across space and seasons. Positive offset values thus indicate, on average, warmer forest microclimate conditions, whereas negative values point to a colder forest microclimate. **First, we calculated the daily mean temperature offset, which corresponds to the difference between the daily mean microclimate temperature, as measured by the loggers, and the corresponding daily**



mean air temperature value at 2 m height for exactly the same month, year and grid cell from EOBS data with a spatial resolution of 1 km<sup>2</sup> (Cruz-alonso et al., 2022). Moreover, the EOBS data underwent an altitudinal correction according to the lapse rate of that grid cell (Karger et al., 2022). Finally, the daily temperature offset values were aggregated into monthly offset values.

#### Acquisition of covariate layers

Covariates were selected based on their known relevance for forest microclimatic temperatures according to literature (Greiser et al., 2018; Zellweger et al., 2019), spatial resolution and availability at the continental scale. In total, twenty covariate layers were selected to create a covariate layer stack, including topographical, biological and macroclimatic variables.

Topographic layers were derived from a digital elevation model (EU-DEM v1.1) at 25 m resolution (European Union, 2020). Both northness and eastness were derived as the cosine and sine of the aspect (°), respectively. Additionally, we incorporated slope (°), elevation (m a.s.l.) and latitude to account for the variation in incoming solar radiation (Lenoir & Svenning, 2013; Meineri & Hylander, 2017). Relative elevation (m) represents the elevational difference between each pixel and the lowest pixel within a 500 m buffer. This is often used as a proxy for cold air drainage, as cold air moves downslope (Ashcroft & Gollan, 2013). Distance to the coast was included because the heat capacity of the ocean has an important effect on (microclimatic) temperatures (Vercauteren, Destouni, Dahlberg, & Hylander, 2013; Zellweger et al., 2019). Furthermore, the effect of increased water vapour content in the atmosphere near the coast affects cloud patterns which, in turn, influence incoming solar radiation (Zellweger et al., 2019). Finally, the topographic wetness index (TWI) was used as a proxy for soil moisture (Meineri, Dahlberg, & Hylander, 2015). This index quantifies the effect of topographic variation on hydrological processes by taking into account both slope and specific catchment area (Beven & Kirkby, 1979). We calculated TWI by using the *Freeman FD8* flow algorithm with a flow dispersion of 1.0, a flow width equal to the raster cell size (i.e. 25 m) and a local slope gradient (Kopecký, Macek, & Wild, 2021).

The 2015 high resolution (20 m) Copernicus maps of tree cover density (%), referring to the percentage of tree cover per raster cell, and forest type (broadleaf vs. coniferous) were included. To quantitatively capture the phenological differences between broadleaved and coniferous forests, we calculated two NDVI values, representative for winter (December-February) and summer months (June-August). NDVI variables were derived from Landsat 4, 5, 7 and 8 satellite images over a period from 2000-2020 provided in Google Earth Engine (Gorelick et al., 2017). Each image underwent pre-processing by converting low-quality data (e.g. due to presence of clouds, snow or shadows) into missing values based on the masks provided with the downloaded images.

Furthermore, long-term average macroclimatic conditions were considered by including four WorldClim bioclimatic variables covering the period between 1970 and 2000 (Fick & Hijmans, 2017): BIO1 (Mean Annual Temperature), BIO5 (Maximum Temperature of the Warmest Month), BIO6 (Minimum Temperature of the Coldest Month) and BIO12 (Annual Precipitation). These were chosen due to the specific interaction of these variables with some of the topographical and biological variables. For instance, Greiser et al. (2018) found that forest density was an important driver for minimum and maximum microclimate temperatures in summer, whereas topography had a stronger influence on extreme temperatures in autumn and winter. Furthermore, mean annual cloud cover (%) over 2000-2014 derived from MODIS products was included to account for the effect of cloud cover on incoming solar radiation (Wilson & Jetz, 2016). Annual snow cover probability (%) was derived as the average of monthly snow probability based on a pixel-wise frequency of snow occurrence (snow cover > 10%) in MODIS daily snow cover products (MOD10A1 & MYD10A1; Hall, Riggs, Salomonson, DiGirolamo, & Bayr, 2002) over 2001-2019. Finally, we also included the sensor height above the ground surface as a covariate in our models, as this significantly impacts the magnitude of the temperature offset (De Frenne et al., 2019; Geiger, 1950).

When necessary, covariate map layers were reprojected and resampled to an equal area projection in EPSG:3035 (ETRS89-extended / LAEA Europe) at 25 m resolution using bilinear interpolation for quantitative data and the nearest neighbour method for categorical data. We present variable importance quantitatively and the relationship between each covariate and the response visually in partial dependence plots (Figure S2). Furthermore, we show the strongest two- and three-way interactions among covariates (Figure S3).

### **Geospatial modelling**

Machine-learning techniques often outperform other statistical techniques such as generalized linear models (GLMs) or generalized additive models (GAMs) in terms of predictive power (Appelhans, Mwangomo, Hardy, Hemp, & Nauss, 2015). As we aim to maximize predictive power within the environmental space covered by our data rather than explanatory power, we used boosted regression trees (BRTs), also referred to as gradient boosting machine, to model the relationship between the selected covariates and  $\Delta T$  (Appelhans et al., 2015; Elith, Leathwick, & Hastie, 2008). Especially for regression, BRTs are particularly valuable due to their capacity to uncover nonlinear relationships as well as their automatic detection of complex interactions among covariates (Figure S3). Furthermore, this algorithm is capable to handle multicollinearity among covariates (Figure S4), outliers and missing data. On the other hand, BRTs are prone to (i) overfitting due to sequential fitting of trees (Elith et al., 2008) and (ii) errors when extrapolating outside the boundaries of the training data. To deal with these issues, we (i) implemented model regularization by means of low learning rate values (0.1-0.001) and

cross-validation (Elith et al., 2008) and by (ii) providing a map indicating where the model is extrapolating beyond the values of the training data.

BRTs were built using the *gbm* R package (Ridgeway, 2005). We searched for the optimal hyperparameter values with the *caret* package (Kuhn, 2012) by means of a grid search over the possible values of the four hyperparameters: interaction depth (2-6); total number of trees (100-10,000); learning rate (0.1-0.001); and the minimal observations in each terminal node (8-12) (Elith et al., 2008). In total, 14,925 models were evaluated by 10-fold cross-validation (CV) while (i) taking into account logger ID to avoid pseudo-replication between folds and (ii) stratifying by the biogeographical regions of Europe (Cervellini et al., 2020), meaning that each fold contained 10% of the loggers in each biogeographical region. Finally, **optimal hyperparameters were selected according to the trade-off between model performance ( $R^2_{cv}$ ) and computational time.**

Once the optimal hyperparameter values were determined, we applied a stratified bootstrap approach to fit 30 different models (van den Hoogen et al., 2019). The bootstrapping procedure randomly sampled the data each time with replacement to fit the model. The biogeographical regions of Europe (Cervellini et al., 2020) were used as stratum for the random sampling to ensure that every biogeographical region was proportionally represented according to data availability in each region. Each of the bootstrapped models made separate predictions for each month – that is 3,141,115,825 European forest pixels classified 360 times (12 months  $\times$  30 bootstraps). Model precision was then quantified by calculating, per pixel, a 95% confidence interval (mean  $\pm$  1.96 SE) for each month. We predicted temperature at 15 cm height as this is the most common height within the input data (Table S2). Furthermore, most understory forest plant species (e.g. herbs, grasses, sedges and ferns) fit, on average, to this height.

Machine-learning techniques, like BRTs, are known to be less capable in extrapolating beyond the boundaries set by the environmental variables in the original training data. To assess where our model is extrapolating – and thus possibly providing less reliable predictions – we calculated for each pixel the percentage of quantitative covariate layers for which the pixel value lies outside the range of data covered by the dataset. Finally, we used a spatial leave-one-out cross-validation analysis to test the effect of spatial autocorrelation in the dataset (Figure S5; Roberts et al., 2017; van den Hoogen et al., 2021). This approach each time validates a model on data from one distinct location and trains a model on the remaining data. This is repeatedly done for each of our **1,197** locations. Because of potential spatial autocorrelation close to the validation location, this process is repeated with an increasing buffer around the validation location, each time excluding data points that fall within the defined buffer zone from the training data. This method allows assessing the influence of spatial autocorrelation on the  $R^2$ .

## **Offset and forest microclimate temperature maps at 25 m resolution**

Here, we make the European monthly temperature offset grids available as open data. These can, in turn, be used to convert gridded macroclimate products into gridded microclimate products. We opted to illustrate the calculation of the mean annual forest microclimatic temperature (further referred to as “forestBIO1”) but this calculation can be carried out for all other temperature-related bioclimatic variables from BIO1 to BIO11 (Fick & Hijmans, 2017; Dirk Nikolaus Karger et al., 2017). First, we calculated (i) the mean annual temperature offset as the average of the monthly offset maps and (ii) the mean annual temperature over 2000-2019 from monthly TerraClimate data (Abatzoglou et al., 2018). Second, we calculated forestBIO1 by adding anomalies of the predicted mean annual offset to the corresponding TerraClimate mean annual temperature map (Abatzoglou et al., 2018).

All calculations were performed in R version 4.0.2 (R Core Team, 2020). The *Tier-2 Genius* cluster from the high-performance computing facilities of Flanders was used to perform the calculations.

## RESULTS AND DISCUSSION

### ForestTemp – microclimatic temperature maps of European forests

Our bootstrapped models for the monthly temperature offset performed well with a coefficient of determination ( $R^2$ ) of **0.81 (95% CI: 0.80-0.82)**, a root mean square error of **0.59 (0.58°C – 0.60°C)** and a mean absolute error of **0.38 (0.37°C – 0.39°C)**. The spatial leave-one-out cross-validation **showed reasonable predictive performance with  $R^2$  stabilizing around 0.40** when increasing the buffer size above 100 km (Figure S5). Mean monthly temperature offsets at 15 cm above ground over 30 bootstrap iterations ranged between **-3.3°C and 8.1°C in January and from -6.3 to 5.4°C in July** (Table S3). Model predictions described expected patterns in  $\Delta T$ , with forest microclimates overall being warmer than the macroclimate during winter and colder during summer (Figure 1). This corresponds to earlier findings for temperate systems, where forests act as a thermal insulator: on average cooling the understory by **0.6°C** in summer and warming it by **1.0°C** in winter compared to monthly free-air temperature (De Frenne et al., 2019; Geiger, 1950; Zellweger et al., 2019). Our model was also able to capture the phenological difference between broadleaved and coniferous forests. We found bimodal peaks in winter, particularly pronounced in January (Figure 2), with temperature offsets in coniferous forests, on average, 1.0°C warmer (Figure S6). This likely relates to the differences in tree cover density between these two forest types during that time of year. The observed pattern can further be caused by the fact that coniferous forests are, at the continental scale, more abundant in places with snow, which is known to act as an additional thermal insulator (Aalto, Scherrer, Lenoir, Guisan, & Luoto, 2018). Mean annual temperature offsets ranged between **-4.0°C and 4.3°C**, which translate into a mean annual forest microclimate temperature (forestBIO1) between **-2.9°C and 22.0°C** across Europe (Figure 3), compared to mean annual macroclimate temperature ranging between -3.5°C and 20.4°C.

The bootstrapped models turned out robust, as standard errors were generally small compared to the modelled temperature offsets: standard errors of the mean of monthly temperature offsets stayed below **0.7°C** in most months (**with the exception of January and November**) and across most parts of Europe (Figure 4, Table S3). Higher standard errors are noticed when predicting the offset at very high (above mid-Sweden) and very low latitudes (southern Spain) as well as in high-elevational regions, which are expected to be caused by extrapolation outside the environmental gradient covered by the availability of temperature loggers installed in forest ecosystems (Figure 5a; Figure S1b). The overall precision of each prediction is represented by the width of the 95% confidence interval for each pixel (Figure 5b), which maximally reaches **4.4°C in winter (January) and 2.1°C in summer** (July, Table S3).

As for any other machine learning technique, we caution against the use of data from regions where the model is extrapolating (mainly in southern Spain, high elevations areas of the Alps and Scandinavia, Figure 5a). As with any spatial model, our model is calibrated on certain environmental conditions and predictions outside these conditions might induce errors. This problem partly stems from undersampled regions in the database (e.g. southern Spain, the United Kingdom, large parts of eastern Europe and high-elevation forested areas), which should be a scope of future research. The extrapolation (Figure 5a) and precision (Figure 5b) maps could therefore be used as spatial masks to remove or downweight the pixels for which predictions are beyond the range of values covered by the models or unprecise.

### Drivers of microclimate

As expected, seasonality (i.e. month of the year) plays a crucial role in defining the direction of the monthly temperature offset, overall being positive in winter and negative during spring summer and autumn (Figure S2). **Bioclimatic variables seem to be important covariates as well, where** we notice an overall negative relationship between the offset and mean annual temperature (Figure S2), which might be related to the predicted decoupling of forest microclimate warming from warming of the free air (De Frenne et al., 2019; Lenoir et al., 2017). However, global warming-related disturbances like extreme droughts, pest outbreaks (e.g. pathogens, bark beetles) and increased fire incidence could nullify the insulation capacity of the forest canopy under changing conditions, disrupting this low coupling. Furthermore, the high importance of distance to the coast **and intermediate importance of** mean annual precipitation suggest an important role for water (McLaughlin et al., 2017). On the one hand, temperature buffering is a function of local soil moisture, which in turn can be driven by distance to water bodies and precipitation (Davis, Dobrowski, Holden, Higuera, & Abatzoglou, 2019). For instance, it is the effect of increased water vapour content in the atmosphere near the coast which affects cloudiness, which in turn is an important variable as it affects shading and incoming solar radiation. On the other hand, moisture can have an impact in different ways, e.g. by increasing the vegetation or snow cover. **Although snow cover is not coming forward as one of the most important covariates, snow is known to be important in driving the temperature offset (Aalto et al., 2018). We expect that the temporal and spatial resolution of this data is too coarse to capture the effect of snow cover. However, the interaction between sensor height, month and latitude (Figure S3b) could hint** towards an insulating effect of snow on the sensor which is, contrary to standardised meteorological stations, not kept free of snow or ice. We thus expect that large positive wintertime offsets in regions with high snow cover probability (i.e. high-latitudinal and high-elevational regions) are mainly caused by this snow insulation effect. Of moderate importance are topographic variables such as slope and elevation, which **both** show a negative relationship with  $\Delta T$ .

Surprisingly, biotic variables such as tree cover density or forest type seem to be less good predictors for the offset at the continental scale. However, the spatial resolution of 25 m used here is probably still too coarse to fully capture these effects (Kašpar et al., 2021). Importantly, the availability of accurate stand-level data at 25 m resolution (e.g. basal area, stem density, leaf area density or tree height) is still limited. Spaceborne, airborne or terrestrial LiDAR-derived variables could be a valuable source of data to solve such issues in the future (Frey et al., 2016; George et al., 2015; Kašpar et al., 2021). However, just as with mean annual temperature, these effects might already be partially captured by or confounded with the combination of seasonality and NDVI.

Note that we do not intend to unravel the physical mechanisms driving the offset between forest microclimate temperatures and free-air temperature. We are aware that most of our explanatory variables (e.g. tree cover density, northness or slope) are indirect drivers and rather affect the physical mechanisms driving the offset (e.g. incoming solar radiation, wind speed) than sub-canopy temperatures directly (Bennie, Huntley, Wiltshire, Hill, & Baxter, 2008). However, as we aim to create continental high-resolution sub-canopy temperature maps for understory vegetation in European forests, a few strong correlative relationships could be better than complex, physical models that are computationally difficult to run at the continental extent and at high spatial resolution. Additionally, some potentially important variables are not incorporated within our models, either due to the limited availability or coarse spatial resolution of those variables. One of the possible limitations of our study is the assumption that forests, and their characteristics, are static over time. However, large parts of European forests are managed (Senf & Seidl, 2021), which makes it virtually impossible to incorporate up-to-date vegetation variables such as forest height, basal area or age. Furthermore, although we incorporated snow cover probability in the model, we do need the exact snow height and duration at high spatiotemporal resolution to quantify the insulation effect of snow on the logger sensors at different heights (Gisnås, Westermann, Schuler, Melvold, & Etzelmüller, 2016). Unfortunately, data on snow water equivalent, needed to calculate snow height and duration, are only available at a coarse spatial resolution of 5 km<sup>2</sup>. Incorporating this into the model would not improve the model as there is still high, fine-scale spatial variability within each pixel. In addition, given the strong correlation of fine-scale snow dynamics with topography, inclusion of the latter is likely to partially capture this effect (Aalto et al., 2018; Niittynen & Luoto, 2018).

Finally, the 25 m spatial resolution is a significant step forward compared to existing microclimate products across large spatial extents. Nonetheless, we have to acknowledge the remaining within-pixel variability both in spatial and temporal terms. Moreover, we know that some organisms, depending on their body size, utilize microclimatic variation at orders of magnitude less than the spatiotemporal resolution used in this study. For instance, small insects can use sunflecks

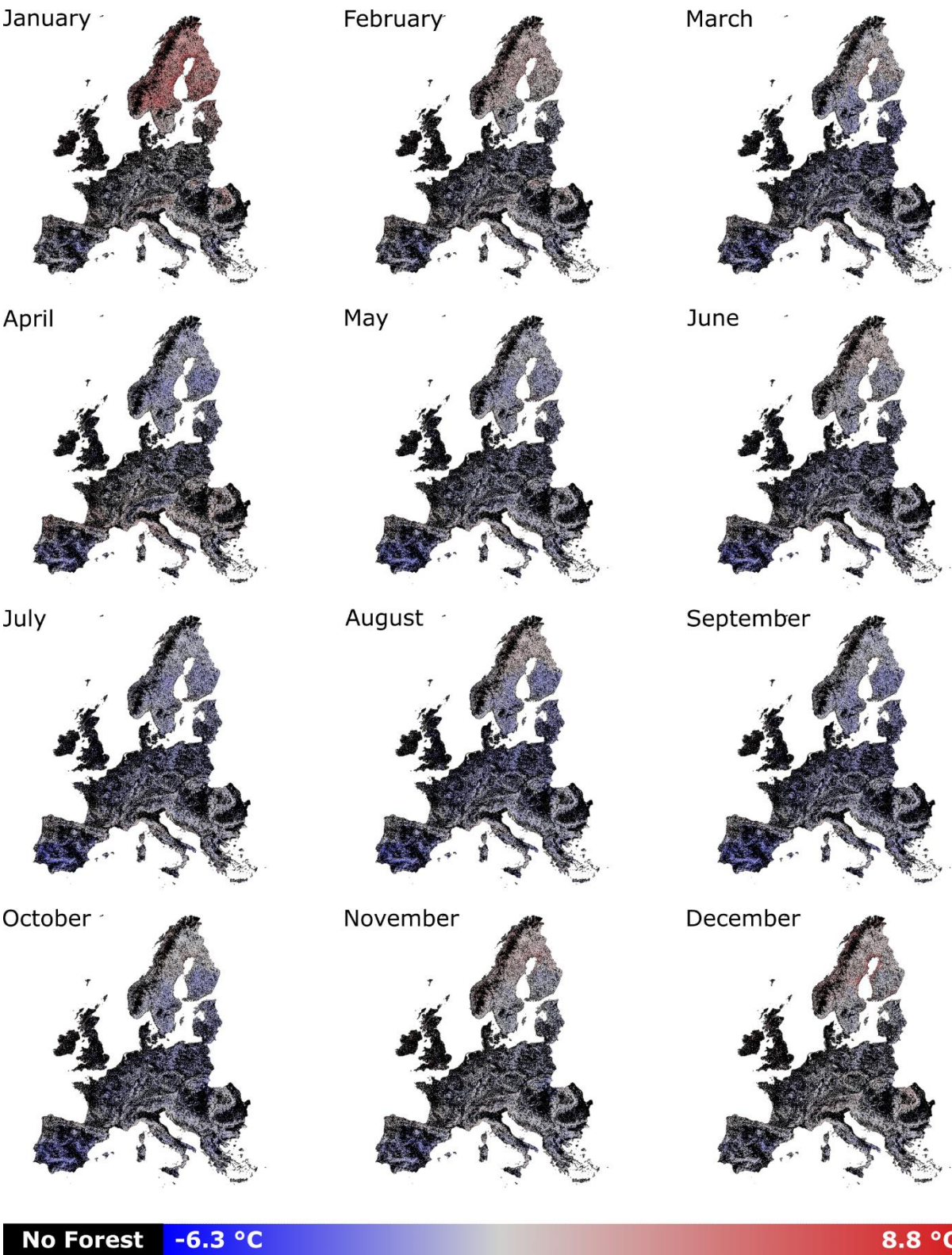
and microhabitats (tree holes and dead wood) available within a 25 m × 25 m grid cell to seek microvariation in temperature throughout the course of the day. Hence, recent research argues in favour of incorporating especially higher temporal resolutions in ecological analyses (Bütikofer et al., 2020). However, given current-day data availability and computational power as well as our focus on the forest floor, this study mapped microclimates at a continental scale according to the state-of-the-art.

### **Applications and future perspectives**

The outcomes of this study allow researchers to use accurate forest microclimate temperature data in large-scale analyses. This is an important step forward as the mismatch between macro- and microclimate forest temperatures is substantial and can seriously bias the outcome of ecological and global change studies. For example, microclimate-informed species distribution models (SDM; Lenoir et al., 2017) could reveal more accurate insights into the various processes underlying species vulnerability to climate change on different aspects, including climate change exposure, sensitivity, adaptability and dispersal (Pacifi et al., 2015). Climate change exposure can be buffered by microclimate whereas climate sensitivity impacts a species' ability to cope with microclimatic warming. Furthermore, microclimatic variation affects the spatial distribution of adaptive genetic variation and thus the ability of a population to survive climate change (De Kort et al., 2020; Graae et al., 2018). Finally, microclimate drives the spatial distribution of dispersal pathways throughout the landscape and thus directly impacts dispersal ability and populations in fragmented landscapes. Understanding how these processes interact with microclimate to shape species responses and their vulnerability to climate change is fundamental to predicting range dynamics.

We trust the predicted thermal offsets for forest ecosystems and their possibility to derive gridded microclimate products will enable future research to more accurately model ecological processes and patterns in the forest understory, as well as forest-dwelling species distributions affected by climate change. These maps are available as GeoTIFFs for download through figshare (doi: 10.6084/m9.figshare.14618235) and will be updated as more or better data become available.





449

450

451

452

**Figure 1: Predicted mean monthly air temperature offset across European forests.** Mean monthly temperature offset at 15 cm above ground between in-situ forest microclimate and free-air temperatures (sub-canopy T°C minus free-air T°C) (in °C).

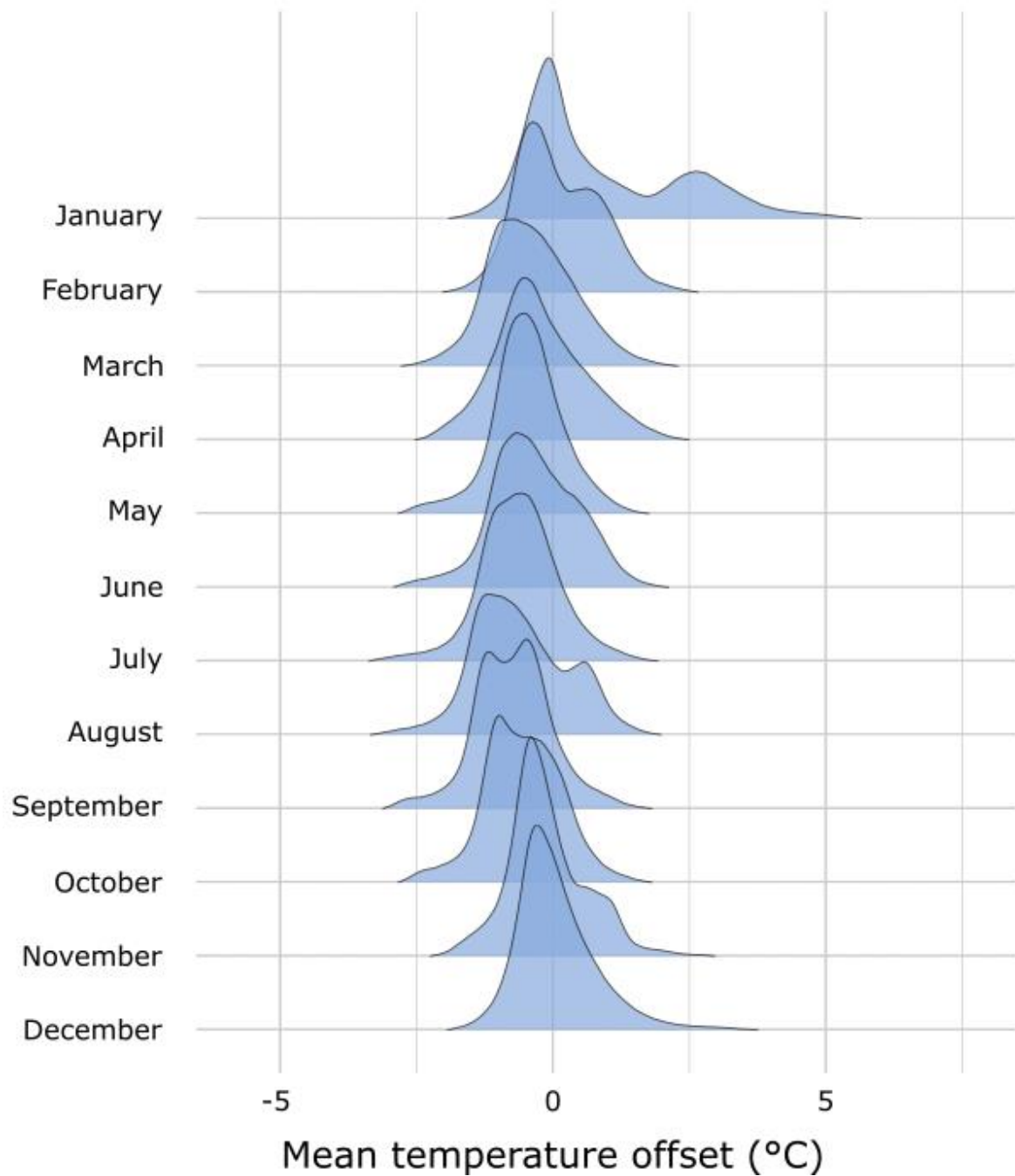


**Figure 2: Histograms of mean monthly temperature offsets.** Density ridgeplots for the monthly temperature offset at 15 cm above ground between in-situ forest microclimate and free-air temperatures (sub-canopy  $T^{\circ}\text{C}$  – free-air  $T^{\circ}\text{C}$ ) (in  $^{\circ}\text{C}$ ) indicating, per month, the distribution of 1,000,000 randomly sampled raster pixel values across European forests.



458

459

460

461

462

**Figure 3: forestBIO1.** Mean annual temperature at 15 cm above ground in European forests (in °C) with a spatial resolution of 25 m, representative of the 2000-2020 period, calculated using the maps of monthly mean air temperature offsets at 25 m resolution (Figure 2) added to the mean annual air temperature from TerraClimate at 4 km resolution.



January



April



July



October



No Forest

0 °C

1.1 °C

**Figure 4: Robustness of the temperature offset model at 15 cm above ground across European forests.** Standard errors of the mean from predicted mean monthly temperature offsets (sub-canopy T°C minus free-air T°C) at 15 cm above ground derived from 30 bootstrapped models (in °C). For additional months, see supplementary Figure 7. See Supplementary Table 3 for detailed quantitative data.

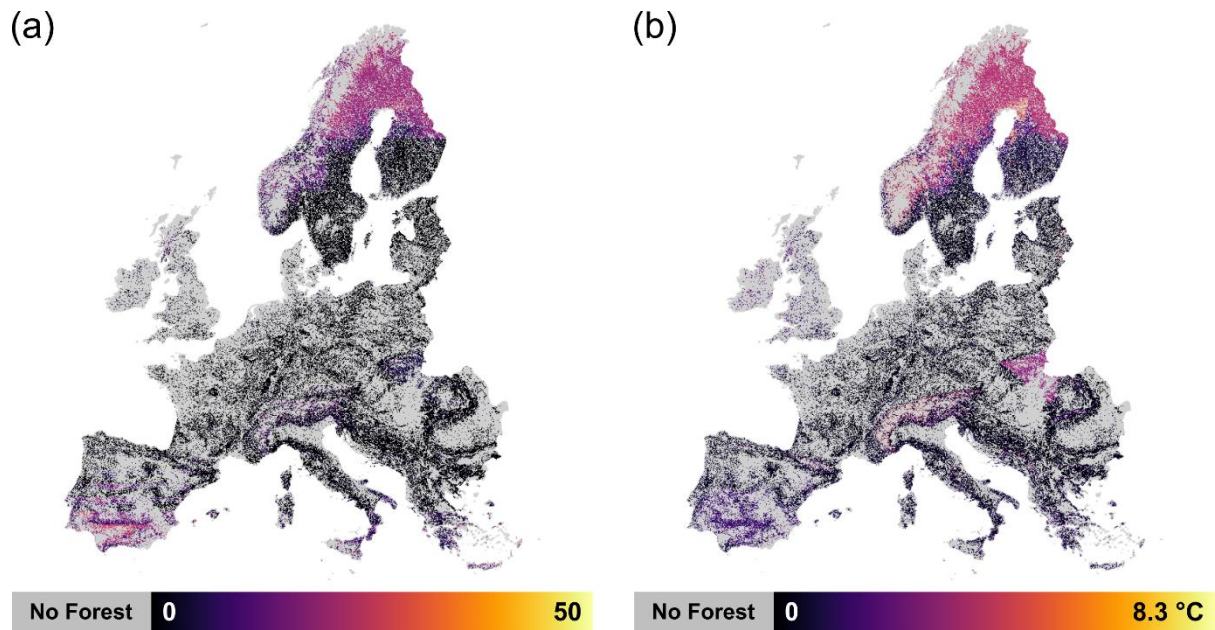


**Figure 5: Extrapolation and precision maps.** (a) The percentage of quantitative variables for which the pixel lies outside the range of data covered by the training data. Pixels with high values indicate that the model has to extrapolate for many of the covariates for that specific pixel (i.e. due to missing in-situ measurements). (b) Precision of predictions for each pixel, calculated as the width of the bootstrapped 95% confidence interval for each pixel.

## ACKNOWLEDGMENTS

SH received funding from a FLOF fellowship of the KU Leuven (project nr. 3E190655). JIL and IN received funding from the Research Foundation Flanders (FWO) (grant nr. WOG W001919N). PDF, PV, EDL and CM received funding from the European Research Council (project FORMICA; <http://www.formica.ugent.be>; grant nr. 757833). JA received funding from the Academy of Finland Flagship (grant nr. 337552) and the University of Helsinki (project MicroClim; grant no. 7510145). MK, MM, JW, LH, JB and MM received funding from the Czech Science Foundation (grant nr. GAČR 20-28119S) and the Czech Academy of Sciences (grant nr. RVO 67985939). JL received funding from: (i) the Agence Nationale de la Recherche (ANR) (project IMPRINT ; grant nr. ANR-19-CE32-0005-01); (ii) the Centre National de la Recherche Scientifique (CNRS) (Défi INFINITI 2018: MORFO); and the Structure Fédérative de Recherche (SFR) Condorcet (FR CNRS 3417: CREUSE). NB and MG received funding from the Swiss National Science Foundation (grant nr. 20FI21\_148992 and grant nr. 20FI20\_173691). SG received funding from the Research Foundation Flanders (FWO) (grant nr. G0H1517N). FM received funding from the Slovak Research and Development Agency (grant nr. APVV-19-0319). AS received funding from ETH Zürich (project FEVER ETH-27 19-1). FZ received funding from the Swiss National Science Foundation (grant no. 193645).

We thank Dr. Wanda De Keersmaecker for her help with the calculations and recommendations concerning the NDVI. JL and FS acknowledge Manuel Nicolas and all forest officers from the Office National des Forêts (ONF) who are in charge of the RENECOFOR network and who provided help and local support for the installation and maintenance of temperature loggers in the field. The computational resources and services used in this work were provided by the VSC (Flemish Supercomputer Center), funded by the Research Foundation Flanders (FWO) and the Flemish Government – department EWI.

**Conflict of Interest:** The authors declare that they have no conflict of interest.

**Data sharing:** The processed input data (i.e. monthly temperature offset values) that support the findings of this study as well as all raster layers (GeoTIFFs) produced in this study are openly available in figshare at <https://doi.org/10.6084/m9.figshare.14618235> while the raw temperature time series necessary to process monthly temperature offset values are available from SoilTemp, a global database of soil and near-surface air temperature measurements data. Restrictions apply to the availability of raw SoilTemp data, which were used under license for this study. The raw temperature time series data are available from Jonas Lembrechts/Stef Haesen with the permission of SoilTemp data contributors of this study.

## REFERENCES

- Aalto, J., Scherrer, D., Lenoir, J., Guisan, A., & Luoto, M. (2018). Biogeophysical controls on soil-atmosphere thermal differences: implications on warming Arctic ecosystems. *Environmental Research Letters*, 13(7), 074003. <https://doi.org/10.1088/1748-9326/aac83e>
- Abatzoglou, J. T., Dobrowski, S. Z., Parks, S. A., & Hegewisch, K. C. (2018). TerraClimate, a high-resolution global dataset of monthly climate and climatic water balance from 1958–2015. *Scientific Data*, 5(1), 170191. <https://doi.org/10.1038/sdata.2017.191>
- Appelhans, T., Mwangomo, E., Hardy, D. R., Hemp, A., & Naus, T. (2015). Evaluating machine learning approaches for the interpolation of monthly air temperature at Mt. Kilimanjaro, Tanzania. *Spatial Statistics*, 14, 91–113. <https://doi.org/10.1016/j.spasta.2015.05.008>
- Ashcroft, M. B., & Gollan, J. R. (2013). The sensitivity of topoclimatic models to fine-scale microclimatic variability and the relevance for ecological studies. *Theoretical and Applied Climatology*, 114(1–2), 281–289. <https://doi.org/10.1007/s00704-013-0841-0>
- Bennie, J., Huntley, B., Wiltshire, A., Hill, M. O., & Baxter, R. (2008). Slope, aspect and climate: Spatially explicit and implicit models of topographic microclimate in chalk grassland. *Ecological Modelling*, 216(1), 47–59. <https://doi.org/10.1016/j.ecolmodel.2008.04.010>
- Beven, K. J., & Kirkby, M. J. (1979). A physically based, variable contributing area model of basin hydrology. *Hydrological Sciences Bulletin*, 24(1), 43–69. <https://doi.org/10.1080/02626667909491834>
- Bramer, I., Anderson, B. J., Bennie, J., Bladon, A. J., De Frenne, P., Hemming, D., ... Gillingham, P. K. (2018). Advances in Monitoring and Modelling Climate at Ecologically Relevant Scales. *Advances in Ecological Research*, 58, 101–161. <https://doi.org/10.1016/BS.AEER.2017.12.005>
- Bütikofer, L., Anderson, K., Bebb, D. P., Bennie, J. J., Early, R. I., & Maclean, I. M. D. (2020). The problem of scale in predicting biological responses to climate. *Global Change Biology*, 26(12), 6657–6666. <https://doi.org/10.1111/gcb.15358>
- Cervellini, M., Zannini, P., Di Musciano, M., Fattorini, S., Jiménez-Alfaro, B., Rocchini, D., ... Chiarucci, A. (2020). A grid-based map for the Biogeographical Regions of Europe. *Biodiversity Data Journal*, 8. <https://doi.org/10.3897/BDJ.8.e53720>
- Cruz-alonso, V., Pucher, C., Ratcliffe, S., Ruiz-benito, P., Astigarraga, J., Neumann, M., ... Rodríguez-sánchez, F. (2022). The easyclimate R package : easy access to high-resolution daily climate data for Europe. <https://doi.org/10.32942/osf.io/mc8uj>**
- Davis, K. T., Dobrowski, S. Z., Holden, Z. A., Higuera, P. E., & Abatzoglou, J. T. (2019). Microclimatic buffering in forests of the future: the role of local water balance. *Ecography*, 42(1), 1–11. <https://doi.org/10.1111/ecog.03836>

540 De Frenne, P., Lenoir, J., Luoto, M., Scheffers, B. R., Zellweger, F., Aalto, J., ... Hylander, K. (2021).  
541 Forest microclimates and climate change: Importance, drivers and future research agenda.  
542 *Global Change Biology*, (November 2020), gcb.15569. <https://doi.org/10.1111/gcb.15569>

543 De Frenne, P., Zellweger, F., Rodríguez-Sánchez, F., Scheffers, B. R., Hylander, K., Luoto, M., ... Lenoir,  
544 J. (2019). Global buffering of temperatures under forest canopies. *Nature Ecology & Evolution*,  
545 3(5), 744–749. <https://doi.org/10.1038/s41559-019-0842-1>

546 De Kort, H., Panis, B., Helsen, K., Douzet, R., Janssens, S. B., & Honnay, O. (2020). Pre-adaptation to  
547 climate change through topography-driven phenotypic plasticity. *Journal of Ecology*, 108(4),  
548 1465–1474. <https://doi.org/10.1111/1365-2745.13365>

549 Elith, J., Leathwick, J. R., & Hastie, T. (2008). A working guide to boosted regression trees. *Journal of*  
550 *Animal Ecology*, 77(4), 802–813. <https://doi.org/10.1111/j.1365-2656.2008.01390.x>

551 European Union. (2020). Copernicus Land Monitoring Service. *European Environment Agency (EEA)*.

552 Fick, S. E., & Hijmans, R. J. (2017). WorldClim 2: new 1-km spatial resolution climate surfaces for  
553 global land areas. *International Journal of Climatology*, 37(12), 4302–4315.  
554 <https://doi.org/10.1002/joc.5086>

555 Frey, S. J. K., Hadley, A. S., Johnson, S. L., Schulze, M., Jones, J. A., & Betts, M. G. (2016). Spatial  
556 models reveal the microclimatic buffering capacity of old-growth forests. *Science Advances*,  
557 2(4), e1501392. <https://doi.org/10.1126/sciadv.1501392>

558 Geiger, R. (1950). *The climate near the ground*. Cambridge, Mass.: Harvard University Press. 482p.  
559 pages.

560 George, A. D., Thompson, F. R., & Faaborg, J. (2015). Using LiDAR and remote microclimate loggers  
561 to downscale near-surface air temperatures for site-level studies. *Remote Sensing Letters*,  
562 6(12), 924–932. <https://doi.org/10.1080/2150704X.2015.1088671>

563 Gislås, K., Westermann, S., Schuler, T. V., Melvold, K., & Etzelmüller, B. (2016). Small-scale variation  
564 of snow in a regional permafrost model. *The Cryosphere*, 10(3), 1201–1215.  
565 <https://doi.org/10.5194/tc-10-1201-2016>

566 Gorelick, N., Hancher, M., Dixon, M., Ilyushchenko, S., Thau, D., & Moore, R. (2017). Google Earth  
567 Engine: Planetary-scale geospatial analysis for everyone. *Remote Sensing of Environment*, 202,  
568 18–27. <https://doi.org/10.1016/j.rse.2017.06.031>

569 Govaert, S., Meeussen, C., Vanneste, T., Bollmann, K., Brunet, J., Cousins, S. A. O., ... De Frenne, P.  
570 (2020). Edge influence on understorey plant communities depends on forest management.  
571 *Journal of Vegetation Science*, 31(2), 281–292. <https://doi.org/10.1111/jvs.12844>

572 Graae, B. J., Vandvik, V., Armbruster, W. S., Eiserhardt, W. L., Svenning, J.-C., Hylander, K., ... Lenoir,  
573 J. (2018). Stay or go – how topographic complexity influences alpine plant population and



community responses to climate change. *Perspectives in Plant Ecology, Evolution and Systematics*, 30(September 2017), 41–50. <https://doi.org/10.1016/j.ppees.2017.09.008>

Greiser, C., Meineri, E., Luoto, M., Ehrlén, J., & Hylander, K. (2018). Monthly microclimate models in a managed boreal forest landscape. *Agricultural and Forest Meteorology*, 250–251(December 2017), 147–158. <https://doi.org/10.1016/j.agrformet.2017.12.252>

Hall, D. K., Riggs, G. A., Salomonson, V. V., DiGirolamo, N. E., & Bayr, K. J. (2002). MODIS snow-cover products. *Remote Sensing of Environment*, 83(1–2), 181–194. [https://doi.org/10.1016/S0034-4257\(02\)00095-0](https://doi.org/10.1016/S0034-4257(02)00095-0)

Jarraud, M. (2008). *Guide to meteorological instruments and methods of observation (WMO-No. 8)*. Geneva, Switzerland: World Meteorological Organisation.

**Karger, D. N., Lange, S., Hari, C., Reyer, C. P. O., & Zimmermann, N. E. (2022). CHELSA-W5E5 v1.0: W5E5 v1.0 downscaled with CHELSA v2.0. ISIMIP Repository. <https://doi.org/https://doi.org/10.48364/ISIMIP.836809.2>**

Karger, Dirk Nikolaus, Conrad, O., Böhner, J., Kawohl, T., Kreft, H., Soria-Auza, R. W., ... Kessler, M. (2017). Climatologies at high resolution for the earth's land surface areas. *Scientific Data*, 4(1), 170122. <https://doi.org/10.1038/sdata.2017.122>

Kašpar, V., Hederová, L., Macek, M., Müllerová, J., Prošek, J., Surový, P., ... Kopecký, M. (2021). Temperature buffering in temperate forests: Comparing microclimate models based on ground measurements with active and passive remote sensing. *Remote Sensing of Environment*, 263, 112522. <https://doi.org/10.1016/j.rse.2021.112522>

Kearney, M. R., & Porter, W. P. (2017). NicheMapR - an R package for biophysical modelling: the microclimate model. *Ecography*, 40(5), 664–674. <https://doi.org/10.1111/ecog.02360>

Kearney, M. R., Shamakhy, A., Tingley, R., Karoly, D. J., Hoffmann, A. A., Briggs, P. R., & Porter, W. P. (2014). Microclimate modelling at macro scales: A test of a general microclimate model integrated with gridded continental-scale soil and weather data. *Methods in Ecology and Evolution*, 5(3), 273–286. <https://doi.org/10.1111/2041-210X.12148>

Kopecký, M., Macek, M., & Wild, J. (2021). Topographic Wetness Index calculation guidelines based on measured soil moisture and plant species composition. *Science of The Total Environment*, 757, 143785. <https://doi.org/10.1016/j.scitotenv.2020.143785>

Körner, C., & Hiltbrunner, E. (2018). The 90 ways to describe plant temperature. *Perspectives in Plant Ecology, Evolution and Systematics*, 30, 16–21. <https://doi.org/10.1016/j.ppees.2017.04.004>

Kuhn, M. (2012). The caret Package. *Journal of Statistical Software*, 28.

Landuyt, D., Perring, M. P., Seidl, R., Taubert, F., Verbeeck, H., & Verheyen, K. (2018). Modelling understorey dynamics in temperate forests under global change—Challenges and perspectives.

- Perspectives in Plant Ecology, Evolution and Systematics*, 31, 44–54.  
<https://doi.org/10.1016/j.ppees.2018.01.002>
- Lembrechts, J. J., Aalto, J., Ashcroft, M. B., De Frenne, P., Kopecký, M., Lenoir, J., ... Nijs, I. (2020). SoilTemp: A global database of near-surface temperature. *Global Change Biology*, (March), gcb.15123. <https://doi.org/10.1111/gcb.15123>
- Lembrechts, J. J., & Lenoir, J. (2020). Microclimatic conditions anywhere at any time! *Global Change Biology*, 26(2), 337–339. <https://doi.org/10.1111/gcb.14942>
- Lembrechts, J. J., Lenoir, J., Roth, N., Hattab, T., Milbau, A., Haider, S., ... Nijs, I. (2019). Comparing temperature data sources for use in species distribution models: From in-situ logging to remote sensing. *Global Ecology and Biogeography*, (August 2018), geb.12974. <https://doi.org/10.1111/geb.12974>
- Lembrechts, J. J., Nijs, I., & Lenoir, J. (2018). Incorporating microclimate into species distribution models. *Ecography*, 1–13. <https://doi.org/10.1111/ecog.03947>
- Lenoir, J., Bertrand, R., Comte, L., Bourgeaud, L., Hattab, T., Murienné, J., & Grenouillet, G. (2020). Species better track climate warming in the oceans than on land. *Nature Ecology & Evolution*, 4(8), 1044–1059. <https://doi.org/10.1038/s41559-020-1198-2>
- Lenoir, J., Graae, B. J., Aarrestad, P. A., Alsos, I. G., Armbruster, W. S., Austrheim, G., ... Svenning, J.-C. (2013). Local temperatures inferred from plant communities suggest strong spatial buffering of climate warming across Northern Europe. *Global Change Biology*, 19(5), 1470–1481. <https://doi.org/10.1111/gcb.12129>
- Lenoir, J., Hattab, T., & Pierre, G. (2017). Climatic microrefugia under anthropogenic climate change: implications for species redistribution. *Ecography*, 40(2), 253–266. <https://doi.org/10.1111/ecog.02788>
- Lenoir, J., & Svenning, J.-C. (2013). Latitudinal and Elevational Range Shifts under Contemporary Climate Change. In *Encyclopedia of Biodiversity* (pp. 599–611). <https://doi.org/10.1016/B978-0-12-384719-5.00375-0>
- Macek, M., Kopecký, M., & Wild, J. (2019). Maximum air temperature controlled by landscape topography affects plant species composition in temperate forests. *Landscape Ecology*, 34(11), 2541–2556. <https://doi.org/10.1007/s10980-019-00903-x>
- Maclean, I. M. D. (2019). Predicting future climate at high spatial and temporal resolution. *Global Change Biology*, (August), gcb.14876. <https://doi.org/10.1111/gcb.14876>
- Maclean, I. M. D., Duffy, J. P., Haesen, S., Govaert, S., De Frenne, P., Vanneste, T., ... Van Meerbeek, K. (2021). On the measurement of microclimate. *Methods in Ecology and Evolution*, 2041-210X.13627. <https://doi.org/10.1111/2041-210X.13627>

642 Maclean, I. M. D., Mosedale, J. R., & Bennie, J. J. (2019). Microclima: An <sc>r</sc> package for  
643 modelling meso- and microclimate. *Methods in Ecology and Evolution*, 10(2), 280–290.  
644 <https://doi.org/10.1111/2041-210X.13093>

645 McLaughlin, B. C., Ackerly, D. D., Klos, P. Z., Natali, J., Dawson, T. E., & Thompson, S. E. (2017).  
646 Hydrologic refugia, plants, and climate change. *Global Change Biology*, 23(8), 2941–2961.  
647 <https://doi.org/10.1111/gcb.13629>

648 Meeussen, C., Govaert, S., Vanneste, T., Haesen, S., Van Meerbeek, K., Bollmann, K., ... De Frenne, P.  
649 (2021). Drivers of carbon stocks in forest edges across Europe. *Science of The Total*  
650 *Environment*, 759, 143497. <https://doi.org/10.1016/j.scitotenv.2020.143497>

651 Meineri, E., Dahlberg, C. J., & Hylander, K. (2015). Using Gaussian Bayesian Networks to disentangle  
652 direct and indirect associations between landscape physiography, environmental variables and  
653 species distribution. *Ecological Modelling*, 313, 127–136.  
654 <https://doi.org/10.1016/j.ecolmodel.2015.06.028>

655 Meineri, E., & Hylander, K. (2017). Fine-grain, large-domain climate models based on climate station  
656 and comprehensive topographic information improve microrefugia detection. *Ecography*,  
657 40(8), 1003–1013. <https://doi.org/10.1111/ecog.02494>

658 Monin, A. S., & Obukhov, A. M. (1954). Basic laws of turbulent mixing in the surface layer of the  
659 atmosphere. *Contrib. Geophys. Inst. Acad. Sci. USSR*, 151(163), e187.

660 Niittynen, P., & Luoto, M. (2018). The importance of snow in species distribution models of arctic  
661 vegetation. *Ecography*, 41(6), 1024–1037. <https://doi.org/10.1111/ecog.03348>

662 Nilsson, M. C., & Wardle, D. A. (2005). Understory vegetation as a forest ecosystem driver: Evidence  
663 from the northern Swedish boreal forest. *Frontiers in Ecology and the Environment*, 3(8), 421–  
664 428. [https://doi.org/10.1890/1540-9295\(2005\)003\[0421:UVAAFE\]2.0.CO;2](https://doi.org/10.1890/1540-9295(2005)003[0421:UVAAFE]2.0.CO;2)

665 Pacifici, M., Foden, W. B., Visconti, P., Watson, J. E. M., Butchart, S. H. M., Kovacs, K. M., ... Rondinini,  
666 C. (2015). Assessing species vulnerability to climate change. *Nature Climate Change*, 5(3), 215–  
667 224. <https://doi.org/10.1038/nclimate2448>

668 Pecl, G. T., Araújo, M. B., Bell, J. D., Blanchard, J., Bonebrake, T. C., Chen, I.-C., ... Williams, S. E.  
669 (2017). Biodiversity redistribution under climate change: Impacts on ecosystems and human  
670 well-being. *Science*, 355(6332), eaai9214. <https://doi.org/10.1126/science.aai9214>

671 Perry, D. A. (1994). *Forest Ecosystems*. Johns Hopkins University Press.

672 Pincebourde, S., & Woods, H. A. (2020). There is plenty of room at the bottom: microclimates drive  
673 insect vulnerability to climate change. *Current Opinion in Insect Science*, 41, 63–70.  
674 <https://doi.org/10.1016/j.cois.2020.07.001>

675 Potter, K. A., Arthur Woods, H., & Pincebourde, S. (2013). Microclimatic challenges in global change

biology. *Global Change Biology*, 19(10), 2932–2939. <https://doi.org/10.1111/gcb.12257>

R Core Team. (2020). *R: A Language and Environment for Statistical Computing*. Vienna, Austria.

Richardson, L. F. (1922). Weather prediction by numerical process. *Cambridge UK: Cambridge University Press*.

Ridgeway, G. (2005). *Generalized boosted models: A guide to the gbm package*.

Roberts, D. R., Bahn, V., Ciuti, S., Boyce, M. S., Elith, J., Guillerá-Arroita, G., ... Dormann, C. F. (2017). Cross-validation strategies for data with temporal, spatial, hierarchical, or phylogenetic structure. *Ecography*, 40(8), 913–929. <https://doi.org/10.1111/ecog.02881>

Scheffers, B. R., De Meester, L., Bridge, T. C. L., Hoffmann, A. A., Pandolfi, J. M., Corlett, R. T., ... Watson, J. E. M. (2016). The broad footprint of climate change from genes to biomes to people. *Science*, 354(6313), aaf7671. <https://doi.org/10.1126/science.aaf7671>

Senf, C., & Seidl, R. (2021). Mapping the forest disturbance regimes of Europe. *Nature Sustainability*, 4(1), 63–70. <https://doi.org/10.1038/s41893-020-00609-y>

van den Hoogen, J., Geisen, S., Routh, D., Ferris, H., Trautspurger, W., Wardle, D. A., ... Crowther, T. W. (2019). Soil nematode abundance and functional group composition at a global scale. *Nature*, 572(7768), 194–198. <https://doi.org/10.1038/s41586-019-1418-6>

van den Hoogen, J., Robmann, N., Routh, D., Lauber, T., van Tiel, N., Danylo, O., & Crowther, T. W. (2021). A geospatial mapping pipeline for ecologists. *BioRxiv*, 1–9. <https://doi.org/10.1101/2021.07.07.451145>

Vercauteren, N., Destouni, G., Dahlberg, C. J., & Hylander, K. (2013). Fine-Resolved, Near-Coastal Spatiotemporal Variation of Temperature in Response to Insolation. *Journal of Applied Meteorology and Climatology*, 52(5), 1208–1220. <https://doi.org/10.1175/JAMC-D-12-0115.1>

Willis, K. J., & Bhagwat, S. A. (2009). Biodiversity and Climate Change. *Science*, 326(5954), 806–807. <https://doi.org/10.1126/science.1178838>

Wilson, A. M., & Jetz, W. (2016). Remotely Sensed High-Resolution Global Cloud Dynamics for Predicting Ecosystem and Biodiversity Distributions. *PLOS Biology*, 14(3), e1002415. <https://doi.org/10.1371/journal.pbio.1002415>

Zellweger, F., Coomes, D., Lenoir, J., Depauw, L., Maes, S. L., Wulf, M., ... De Frenne, P. (2019). Seasonal drivers of understorey temperature buffering in temperate deciduous forests across Europe. *Global Ecology and Biogeography*, 28(12), 1774–1786. <https://doi.org/10.1111/geb.12991>